ADVANCED OPTICAL MATERIALS
www.advopticalmat.de

Progress on Black Phosphorus Photonics

Bingchen Deng, Riccardo Frisenda,* Cheng Li, Xiaolong Chen, Andres Castellanos-Gomez, and Fengnian Xia*

Recent years have witnessed the rapidly growing interests in the rediscovered black phosphorus (BP), an elemental group-V layered material with very high carrier mobility among all semiconducting layered materials. As a layered semiconductor, the bandgap of intrinsic BP varies from ≈0.3 to 2 eV depending on the thickness. This bandgap value can be tuned to below 50 meV by a moderate external electric field. Adsorption doping and external pressure can also effectively modify its bandgap. The largely tunable bandgap of BP makes it a promising material for infrared optics. Moreover, its unique puckered structure leads to the anisotropic in-plane properties, making it ideal for the exploration of exotic physical phenomena and the realization of novel devices. Here, the fundamental optical properties are reviewed and latest developments on BP photonic and optoelectronic devices are discussed.

1. Introduction

Black phosphorus (BP), the most stable allotrope of phosphorus, is an old semiconducting material first synthesized more than one hundred years ago,[1,2] yet it emerges recently as a rediscovered layered 2D material which holds great promise for future electronics and photonics.[3–14] Similar to all the other 2D materials, it is possible to exfoliate few-layer and thin film BP from its bulk crystal, owing to the weak van der Waals interaction among the layers (see BP crystal structure in **Figure 1**a).[3–6] Interestingly, black phosphorus covers a wavelength range which cannot be widely accessed by other layered materials.[15] Graphene has a zero bandgap, and electronic devices made out of graphene cannot be effective turned "off."[16–19] Due to its monolayer nature, the interaction between light and graphene is weak, although it is extremely strong if normalized to its atomic thickness.[15,20–22] Also, because graphene is semimetallic, the optoelectronic devices suffer from large dark current, and therefore high noise level and high power consumption.[23–27] The bandgaps of semiconducting transition metal dichalcogenides (TMDCs) are in general in the range of ≈1–2 eV, leading to limited optical response in technically critical infrared wavelength range.[15,28] Few-layer TMDCs, however, as long as they are thicker than monolayer, are no longer direct bandgap semiconductors.[29,30] Hexagonal-boron nitride (h-BN) has a bandgap of about 6 eV, therefore it is an insulator.[15,31] Black phosphorus provides an opportunity to cover the near and mid-infrared wavelength range. In its bulk form, black phosphorus has a bandgap of ≈0.3 eV.[2–6] This value increases as the thickness of BP thin film goes down, and finally reaches ≈2 eV for the monolayer due the vertical quantum confinement effect, which is a common phenomenon for many semiconducting layered materials.[9,32,33] It is also worth noticing that the bandgap is direct regardless of its thickness.[8,9] The finite bandgap is critical for electronic devices, since it ensures high on–off ratio for a transistor,[3] and significantly reduces dark current.[34] For optical applications, the 0.3 eV direct bandgap makes BP interact strongly with mid-infrared photons and those with even higher energy.[5] Moreover, it was discovered recently that the bandgap of thin-film BP can be efficiently tuned simply by an electrical gating approach, which may allow for the exploration of new physical phenomena and enable more device applications.[35–41] Another distinct feature of black phosphorus is the strong in-plane anisotropy, which originates from the puckered arrangement of phosphorus atoms (shown in Figure 1a).[5] This reduced symmetry results in specific optical transition rules in the momentum space and thus linear dichroic optical properties.[8,42] Due to these desirable properties, a few proof-of-concept devices have been demonstrated with various functionalities.[3,43–50] Toward the practical applications of BP, long-term stability is highly desirable. Although naked black phosphorus can oxidize under ambient environment,[7,51] researchers have developed a number of encapsulation and surface passivation schemes to dramatically improve its long term stability.[52–56] Large-scale controllable production of BP thin film is still at its infancy; nevertheless, encouraging progress is being continuously made.[57–59] In this review, we will also discuss the BP synthesis, since it is critical for future BP applications in photonics.

B. Deng, C. Li, Dr. X. Chen, Dr. F. Xia
Department of Electrical Engineering
Yale University
New Haven, CT 06511, USA
E-mail: bingchen.deng@yale.edu
Dr. R. Frisenda
Instituto Madrileño de Estudios Avanzados en Nanociencia (IMDEA-Nanociencia)
Campus de Cantoblanco
E-28049 Madrid, Spain
E-mail: riccardo.frisenda@imdea.org
Dr. A. Castellanos-Gomez
Materials Science Factory
Instituto de Ciencia de Materiales de Madrid (ICMM-CSIC)
E-28049 Madrid, Spain
The ORCID identification number(s) for the author(s) of this article can be found under https://doi.org/10.1002/adom.201800365.

DOI: 10.1002/adom.201800365

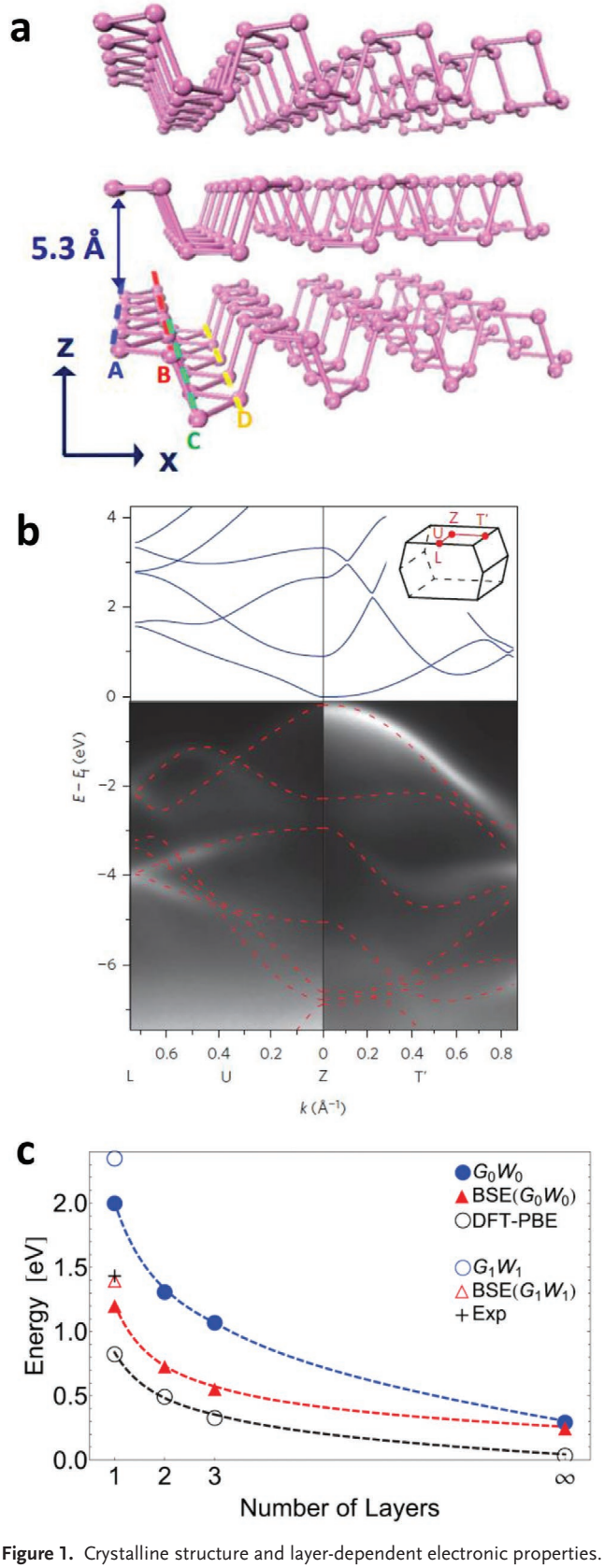

Figure 1. Crystalline structure and layer-dependent electronic properties. a) Schematic of BP crystal, featured by puckered arrangement of phosphorus atoms. Adapted with permission.[10] Copyright 2015, National Academy of Sciences. b) The band structure of bulk BP measured by ARPES. Adapted with permission.[3] Copyright 2014, Springer Nature. c) The bandgap energy of black phosphorus as a function of layer number. GW method calculates the quasiparticle bandgap (electrical bandgap) while BSE method accounts for the optical bandgap. The difference between the electrical gap and optical gap is just the exciton binding energy. Adapted with permission.[9] Copyright 2014, American Physical Society.

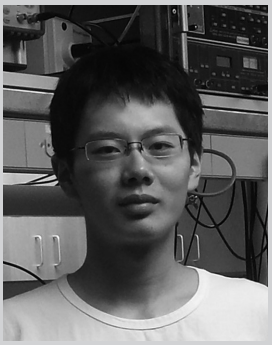

Bingchen Deng is currently a Ph.D. student under the supervision of Prof. Fengnian Xia at Yale University. He received his B.S. degree in physics from University of Science and Technology of China (USTC) in 2014. His research interests include electronics, optoelectronics, plasmonics, and valleytronics in 2D materials.

Riccardo Frisenda is a postdoc in the 2D Materials & Devices research group at IMDEA Nanoscience Research Institute of Madrid. His research in experimental condensed matter physics in particular focuses on the study of optoelectronic nanodevices based on 2D materials. He obtained his Ph.D. in January 2016 at the Kavli Institute of Nanoscience in Delft University of Technology. Since April 2016, he joined the 2D Materials & Devices research group as a Rubicon-fellow postdoc.

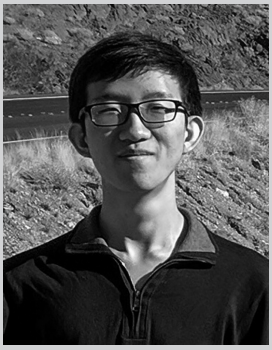

Cheng Li is a Ph.D. candidate in the Laboratory of Emerging Materials and Devices in Yale University, New Haven, USA. His research interests include microelectronic devices and 2D materials. He obtained B.Eng. at Institute of Microelectronics in Tsinghua University, Beijing, China. He joined Laboratory of Emerging Materials and Devices since September 2015.

2. Electronic Properties

The desirable properties of BP originate from its electronic band structure. The band structure of bulk BP measured by

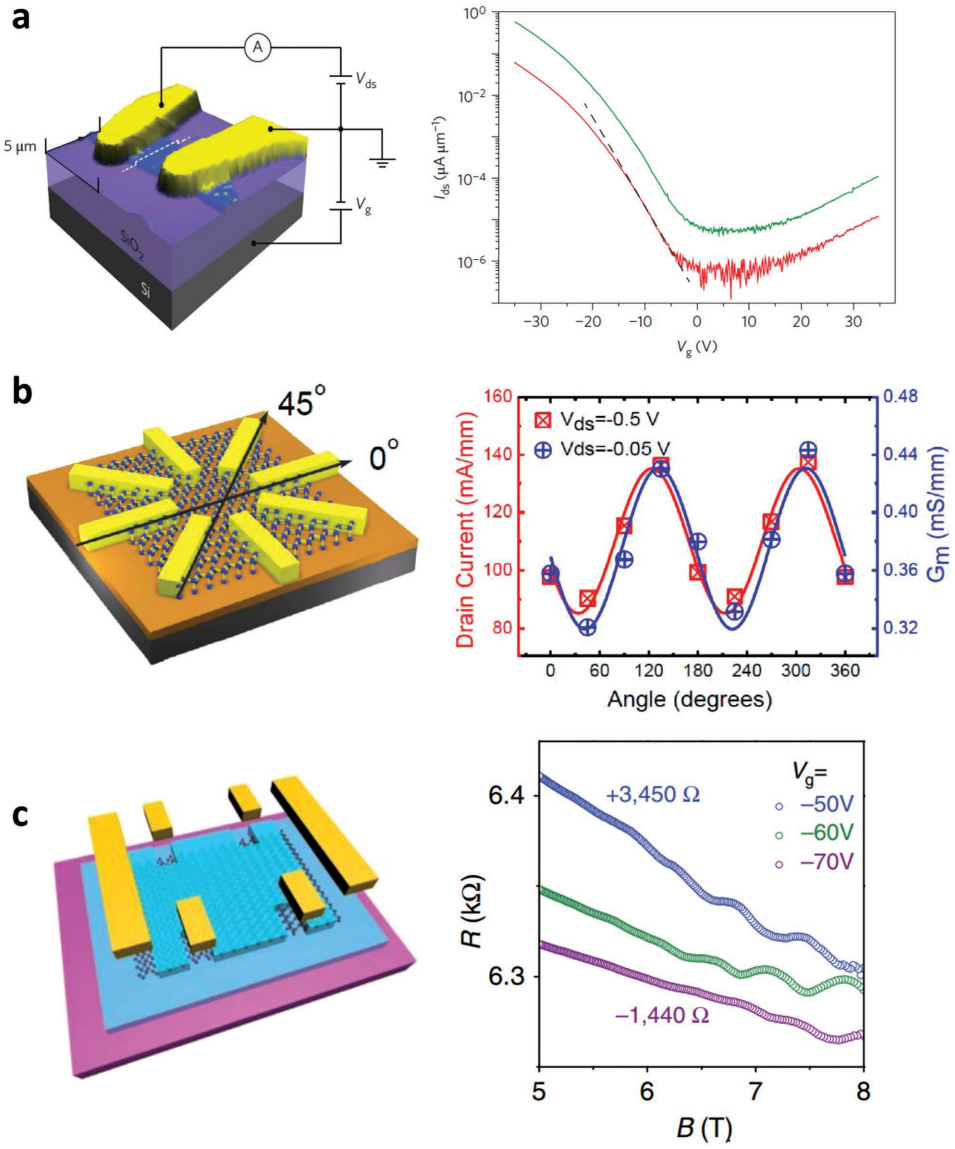

Figure 2. Black phosphorus electronic devices. a) Left: Schematic of the first BP field-effect transistor. Right: Transfer characteristic of the BP FET. Red (green) curve corresponds to a source–drain bias of 10 mV (100 mV). Adapted with permission.[3] Copyright 2014, Springer Nature. b) Left: Device geometry to measure the anisotropy of BP electrical conductivity. Right: Drain current and transconductance as a function of measuring angle. Adapted with permission.[4] Copyright 2014, American Chemical Society. c) Left: Fabrication of fully encapsulated BP device based on h-BN/BP/h-BN heterostructure. Right: Shubnikov–de Haas oscillations observed in high-mobility BP device. Adapted under the terms of the Creative Commons Attribution 4.0 International License.[64] Copyright 2015, Springer Nature.

angle-resolved photoemission spectroscopy (ARPES) together with ab initio calculations is shown in Figure 1b.[3] A ≈0.3 eV direct bandgap is visible at the Z point of the first Brillouin zone. Another interesting feature is that the band dispersion along the *Z*–*U* direction differs from that along the *Z*–*T*′ direction, leading to the different effective masses along the *x*-(armchair) and *y*-(zigzag) directions of the crystal, which causes the strong in-plane anisotropy as will be discussed later. Although the bandgaps of 2D materials in general increase, as the films become thinner because of the quantum confinement effect, the increase in black phosphorus is significant (from ≈0.3 for bulk to 2 eV for monolayer) due the stronger interlayer electronic-state coupling compared with other layered materials such as molybdenum disulfide.[9,35,60] Figure 1c denotes how the bandgap of BP evolves as the function of layer number calculated based on density functional theory.[9]

In 2014, Li et al. first mapped out the band structure of BP using ARPES and constructed first field-effect transistors (FETs) on 5–10 nm thick BP channels.[3] They obtained satisfactory ambipolar FET performance with channel current modulation up to 10^5 together with a field-effect mobility up to 1000 cm^2 V^{-1} s^{-1}. **Figure 2**a shows the first BP thin-film transistor and its transfer characteristic curves. Metal–insulator phase transition at high doping level was observed. Liu et al. studied the device behavior of BP FETs and revealed the unique anisotropic transport properties.[4] Figure 2b shows the angle-dependent transport behavior.

Current saturation was obvious from the output characteristic curves in both studies. This together with the high mobility makes BP a possible candidate for radio frequency and logic circuit applications.[43,61] Recently, even higher mobility BP devices were demonstrated by using h-BN as the substrate,[62–65] which was proved to be effective in preserving the intrinsic ultrahigh mobility of graphene.[66,67] This is because h-BN not only serves as an atomically flat surface to minimize the carrier scattering, but also screens the effects of charge traps in SiO_2 dielectric layer.[66] Li et al. placed a BP flake on a h-BN substrate, and the resulting device showed enhanced mobility so that quantum oscillations were observed in the 2D electron gas of black phosphorus.[62] Chen et al. sandwiched a BP flake between two h-BN layers and the device showed much improved performance.[64] Moreover, it was stable in the long term even in the ambient environment, which is critical for practical applications. Figure 2c shows the fully encapsulated BP device and its quantum oscillations. Due to the high carrier mobility, Shubnikov–de Haas oscillations of resistance were clearly seen when the magnetic field $B > 6$ T.[64] Today, the mobility of thin-film BP (≈4 nm thick) has already reached a record of 5200 and 45 000 $cm^2\ V^{-1}\ s^{-1}$ at room and cryogenic temperatures, respectively.[68] This was achieved by carefully assembling h-BN/BP/h-BN sandwich in vacuum (10^{-3} Torr) to minimize the oxidation of BP. Note that the mobility achieved by vacuum-assisted encapsulation was up to one order of magnitude larger than that achieved by encapsulating BP between h-BN flakes under inert gas atmosphere. The encapsulation of BP between inert layers has gradually become a common practice in current BP research if pristine, high-mobility, and long-term air-stable devices are desirable. **Table 1** summarizes the mobility values reported in the literature.

Table 1. Direct comparison between the field effect characteristics of different BP transistors available in the literature. The mobility displayed in the table is measured for hole charge carriers and, if not indicated, extracted through field-effect measurements.

Ref.	Thickness	Mobility ($cm^2\ V^{-1}\ s^{-1}$)	On–off ratio	Temperature
[3]	5–10 nm	1000	10^5	Room temperature (RT)
[4]	5 nm	286	10^4	RT
[62]	10 nm	400	–	RT
		250 (Hall)	–	
		3900	–	<30 K
		2000 (Hall)	–	
[65]	Few-layer	1000 (Hall)	–	RT
		6000 (Hall)	–	<30 K
[64]	5–10 nm	1350	10^5	RT
		2700	–	2 K
[68]	Few-layer	5200	–	RT
		45 000	–	2 K
[5]	15 nm	1000 (*x* direction) (Hall)	–	120 K
		600 (*y* direction) (Hall)	–	
	5 nm	205	10^5	RT
	2 nm	50	5×10^5	

3. Black Phosphorus Photonics

3.1. Fundamental Optical Properties and Linear Dichroism

In 2014, Xia et al. measured the optical properties of thin-film black phosphorus in near and mid-infrared wavelength range.[5] After that, various studies on BP optical properties and relevant applications have been reported. In the work of Xia et al., the authors reported the polarization-resolved optical extinction of a ≈30 nm thick black phosphorus thin film on SiO_2/Si substrate (**Figure 3**a).[5] From the figure, one can immediately obtain the bandgap of the measured BP thin film to be ≈0.3 eV (corresponding to the ≈2400 cm^{-1} extinction rising edge). This value agrees well with that obtained from ARPES,[3] indicating a negligible exciton effect in such thick BP. One also notices that the optical extinction depends on the polarization of the incident light: above the band edge, for the incident light aligned with the *x*-direction (armchair-direction) of the BP thin film, the extinction reaches its maximum while for the light polarized along *y*-direction (zigzag), the extinction decreases. The infrared spectra together with the Raman scattering provide noninvasive methods to quickly determine the crystal orientations of the BP flakes. Apart from the linear dichroism observed near the absorption band edge of BP, the marked in-plane anisotropy of the puckered lattice also yields linear dichroism of BP within the visible range of the electromagnetic spectrum (thus allowing for crystal orientation determination with quick visible range optical microscopy measurements).[69,70] The anisotropy of black phosphorus also manifests itself through light emission. Wang et al. revealed that the photoluminescence (PL) from monolayer BP is always perfectly linearly polarized along the *x*-direction of the flake, regardless of the polarization of the excitation laser (Figure 3b).[71] The optical absorption of black phosphorus thin film should in principle also shows strong linear dichroism, i.e., the absorption of light polarized along the *y*-direction of the crystal should be weaker than that along *x* and this linear dichroism is 100% at band edge. Detailed studies of black phosphorus band structure from the symmetry point of view by Qiao et al. and Yuan et al. showed that at the direct bandgap of BP, the optical transition of states between valence band and conduction band is allowed for *x*-polarized light because the dipole operator in this case is odd.[8,42] However, the transition is symmetry-forbidden for *y*-polarized light. Therefore, the general trend is that the optical absorption for light polarized along the *y*-direction of BP crystal is forbidden at the immediate band edge, but still increases at higher energy, although it will not exceed that for *x*-polarized light. Li et al. and Zhang et al. studied the layer-dependent infrared spectra of few-layer BP samples and their associated electronic structures.[72,73] It was found that the optical extinction (and reflection) spectra of thin-film BP are affected by the underneath substrate. Li et al. and Zhang et al. used thick sapphire substrate (with top h-BN encapsulation) and quartz substrate to eliminate the multiple reflection within the thin oxide layer if SiO_2/Si are used as the substrate. Figure 3c shows the infrared extinction spectra of BP of several representative thicknesses by Zhang et al.

The results of Li et al. and Zhang et al. indeed confirmed the trend the symmetry analysis predicted. However, even sapphire and quartz are not optimal for measuring the infrared

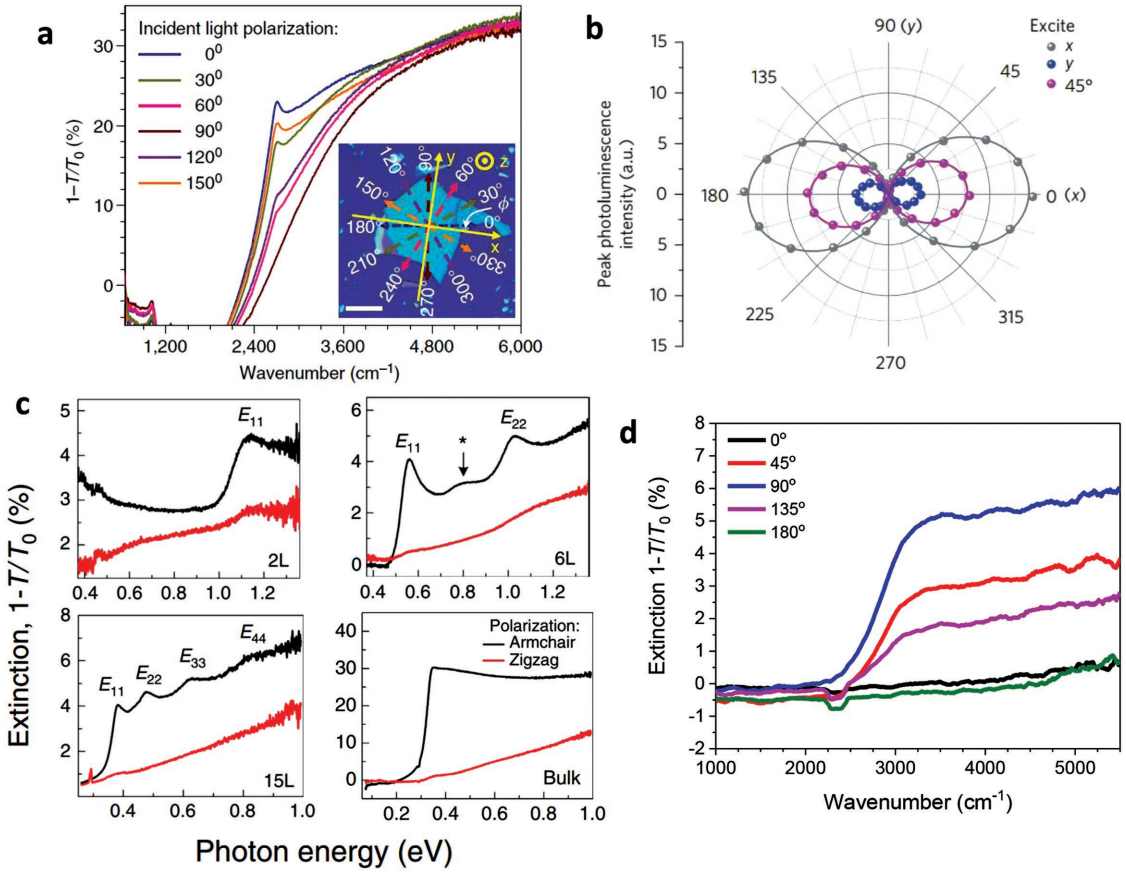

Figure 3. Optical linear dichroism in black phosphorus. a) Polarization-resolved infrared extinction spectra of a ≈30 nm thick BP on 300 nm SiO_2/Si substrate. Inset: The measured flakes with *x*- and *y*-axes denote the armchair and zigzag directions of the BP crystal. Adapted with permission.[5] Copyright 2014, Springer Nature. b) PL intensity as a function of polarization detection angle. Adapted with permission.[71] Copyright 2015, Springer Nature. c) Infrared extinction spectra of BP on quartz with representative thicknesses. For the last panel, the bulk sample (thickness > 100 nm) is on an intrinsic Si substrate. E_{11}, E_{22}, E_{33}, and E_{44} denote the intersubband transitions. Adapted under the terms of the Creative Commons Attribution 4.0 International License.[73] Copyright 2017, Springer Nature. d) Polarization-resolved infrared extinction spectra of a ≈15 nm thick BP sample on ZnS. The 90° in the legend is close to the *x*-direction of the crystal.

extinction spectra of BP due to the following reasons. First, they become less transparent near the bulk BP bandgap energy of ≈0.3 eV and below. Second, they are optically anisotropic themselves. In order to measure the infrared extinction spectra of BP accurately, recently we used a polycrystalline zinc sulfide (ZnS) chip as the substrate. ZnS is transparent in the infrared region up to ≈15 μm (670 cm^{-1}, or 83 meV), and shows isotropic optical transmission during our measurements due to its polycrystalline nature. Figure 3d displays the polarization-resolved extinction spectra of a ≈15 nm thick BP flake on a 1 mm thick ZnS substrate. It is clearly seen that beyond the band edge of 2400 cm^{-1}, the extinctions for different light polarizations diverge, indicating the strong in-plane anisotropy. Several important features are clearly seen: 1) The extinction along the *y*-direction (0° and 180° in the legend) is zero in a very broad energy range. It increases slightly when photon energy exceeds ≈0.6 eV (around ≈5000 cm^{-1} and up). As a result, the linear dichroism is nearly 100% for the measured wavelength range. These observations are consistent with the symmetry argument discussed above.[8,42] 2) The optical extinction for light polarized along the *x*-direction is around 5% for this 15 nm thick sample, which agrees with the theoretical calculation.[74] 3) The extinction rises rapidly first and then increases very slowly, leading to the step-like extinction pattern. This is a reminiscence of optical absorption in a pure 2D system.[32,33] However, the measured sample was 15 nm thick and in such 3D direct bandgap semiconductors we usually expect a $\sqrt{\omega}$-like (ω is the light angular frequency) optical absorption spectrum.[33] For black phosphorus, when it is in 2D form (monolayer), its optical properties are similar to those quasi-1D systems,[71] and correspondingly its bulk form (3D) exhibits 2D-like optical properties. This phenomenon is due to its unique puckered structure.

3.2. Tunable Optical Properties

The optical properties of black phosphorus can be strongly tuned by its thickness, as demonstrated both experimentally[72,73] and theoretically,[9] as discussed above. In the work of Low et al., the authors calculated the optical conductivity of black phosphorus thin film as a function of thickness by using Kubo formula.[74] **Figure 4**a shows their results of BP optical conductivity spectra (real

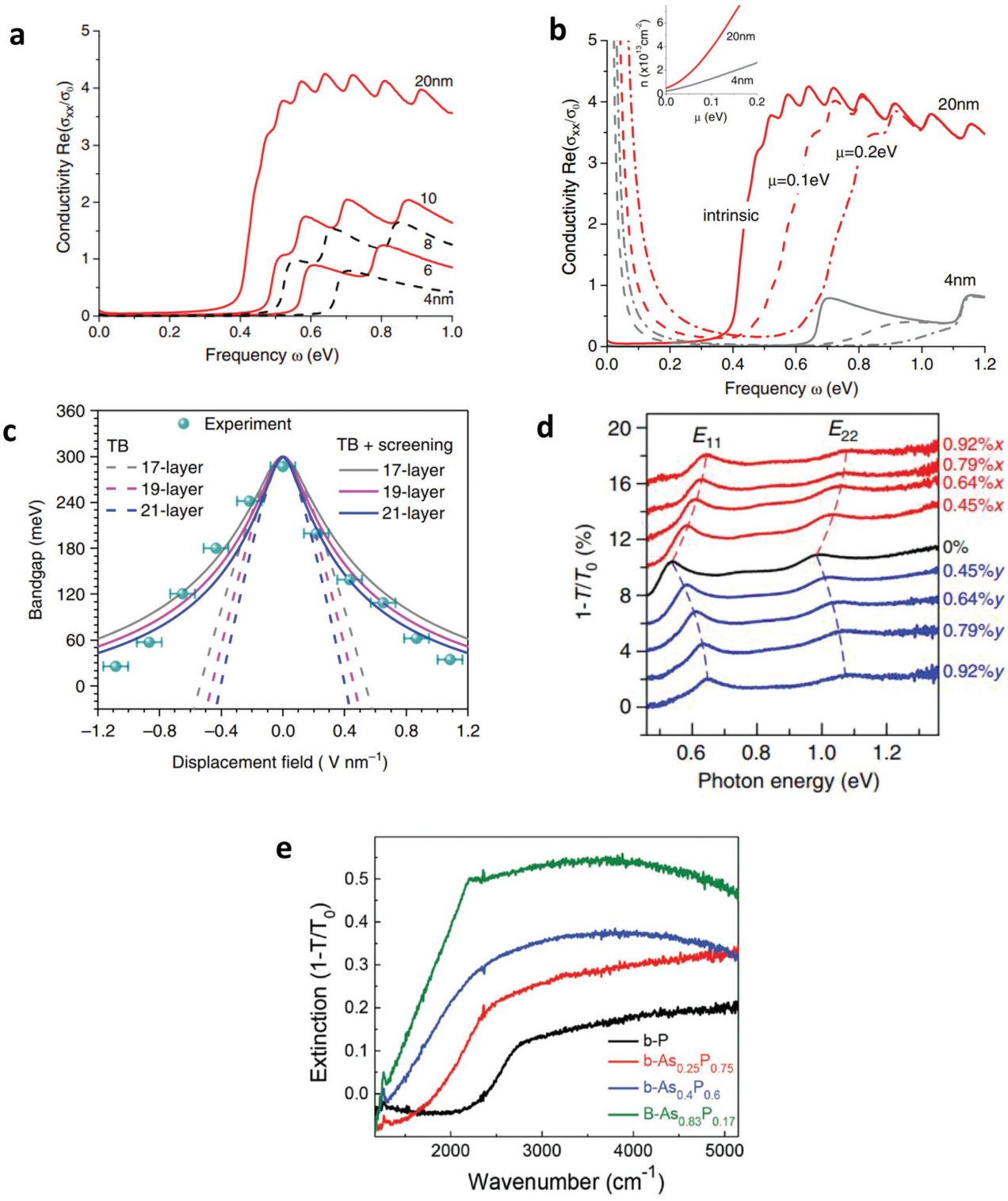

Figure 4. Tuning of black phosphorus optical properties. a) Calculated real part of the optical conductivity along the *x*-direction of BP with different thicknesses. Adapted with permission.[74] Copyright 2014, American Physical Society. b) Calculated real part of the optical conductivity along the *x*-direction of BP with different Fermi levels. Inset: The relationship between carrier concentration and Fermi level. Adapted with permission.[74] Copyright 2014, American Physical Society. c) BP bandgap modulation as a function of vertical displacement field. Dashed (solid) lines: The calculated bandgap tuning properties using the tight-binding model without (with) additional bandgap-dependent dielectric screening effect. Adapted under the terms of the Creative Commons Attribution 4.0 International License.[35] Copyright 2017, Springer Nature. d) Extinction spectra of a 6-layer BP under different tensile strain conditions. E_{11} and E_{22} denote the intersubband transitions. Adapted under the terms of the Creative Commons Attribution 4.0 International License.[73] Copyright 2017, Springer Nature. e) Extinction spectra of b-As_xP_{1-x} with different *x* values. Adapted with permission.[89] Copyright 2015, Wiley-VCH.

part) along the *x*-direction for different thicknesses. As mentioned above, due to the strong linear dichroism, the optical conductivity (real part) along the *y*-direction is close to zero. One major feature in the calculated results is the oscillating patterns in the spectra due to the transitions between different sub-bands. This feature is usually pronounced in 1D system.[32,33,75,76] Here thin-film BP exhibits such properties due to its further "reduced-dimension" nature arising from the puckering of the crystalline structure. Recently Zhang et al. measured the optical extinctions of very thin BP from 2 to 15 layers, and the oscillating behaviors were clearly confirmed (Figure 3c).[73]

Low et al. also theoretically considered the impact of Fermi level (or doping) on the optical conductivity of BP thin film.[74] Figure 4b illustrates that as the Fermi level moves away from the mid-gap, the optical conductivity change exhibits two features. First, the absorption edge undergoes a blue shift due to the Pauli state blocking, similar to that observed in graphene.[22,77,78] Second, as the Fermi level goes higher, the carrier concentration increases, which results in the pronounced free carrier absorption in the low-energy domain.[33,79,80] In the inset of Figure 4b, the authors also calculated the corresponding carrier concentration as a function of Fermi level, which shows that the Fermi levels denoted in Figure 4b are largely accessible.

Other than doping, a vertical electric field applied along the thin film semiconductor material can also tune its optical properties, which is known as the Stark effect.[81] This effect is important for the realization of compact, electrically tunable on-chip optoelectronic devices, such as optical modulators. Previously, III–V quantum wells have been leveraged to build infrared optical modulators based on quantum-confined Stark effect.[82] It is highly desired to uncover and exploit the electric-field tunable bandgap and light absorption in BP. Once achieved, it can extend the operational wavelength range of BP photonic devices to infrared region beyond the intrinsic cut-off wavelength of 3.7 μm (corresponding to the ≈0.33 eV bandgap). Kim et al. first showed that the bandgap of few-layer BP can be tuned and even completely closed through a vertical electric field induced by the adsorption of potassium atoms on the surface.[83] However, although this method is a very effective way to heavily dope the BP to tune its bandgap, from the practical point of view its integration in real-life devices seems extremely cumbersome. Deng et al. recently revealed the detailed thickness-dependent bandgap tuning properties in intrinsic BP thin films by performing transport study on dual-gate BP FETs.[35] Briefly speaking, the bandgap tuning is caused by the potential difference perpendicular to the sample, which is induced by the electric field. However, the strong interlayer coupling limits the bandgap tuning, and the overall bandgap modulation is the result of these two competing factors. They also demonstrated that for BP with a thickness of around 10 nm, the bandgap can be continuously tuned from ≈300 to below 50 meV by a displacement field of ≈1 V nm^{-1}, which can be readily achieved using regular dielectrics. The bandgap value of a 10 nm thick BP as a function of vertical displacement field is shown in Figure 4c. Here the bandgap tuning is very large and is in fact comparable to the bandgap itself. As a result, the screening effect significantly increases as the bandgap shrinks, and the simple tight-binding model alone cannot well explain the experimental results. To account for the additional screening, the bandgap dependent dielectric constant has to be used to model such a large bandgap tuning effect.[35] The similar bandgap tuning effect was also studied by Liu et al. using low-temperature scanning tunneling microscopy.[36] They reported a bandgap reduction from ≈310 to 200 meV through the application of a single back-gate voltage.

Strain also modifies the bandgap of black phosphorus significantly. Quereda et al. investigated BP thin films with periodic rippling structures.[70] By measuring the BP optical absorption at visible range, they indirectly inferred that the optical absorption edges for ripple valleys and ripple summits could differ by 0.7 eV (corresponding to −30% shift for compressive and +10% shift for tensile stress, respectively), which is much larger than its TMDC counterparts. Also in the work of Zhang et al., they directly measured the infrared spectra of BP thin films under strain (Figure 4d).[73] Their results showed that BP was highly sensitive to strain and 1% uniaxial strain could modify the bandgap by more than 20%. Moreover, several experimental[84–86] and theoretical[87,88] works have explored the possibility to tune the electronic band structure of BP through hydrostatic pressure. At moderate pressures BP displays a pressure dependent insulator-to-metal transition[84] and at high pressures BP even undergoes a structural phase transition accompanied by a superconducting transition with a T_c around 5–10 K.[85,86]

Another approach to modify the optical properties of black phosphorus is to alloy BP with arsenic atoms, yielding the black arsenic phosphorus (b-As$_x$P$_{1-x}$) alloy.[89] By adjusting the arsenic concentration in b-As$_x$P$_{1-x}$, the bandgap energy can be reduced down to ≈0.15 eV when x reaches 0.83 while the orthorhombic puckered layered structure is still preserved. The optical absorption edge of b-As$_x$P$_{1-x}$ thus moves to lower frequency when the arsenic concentration increases (Figure 4e). This provides another tuning knob to realize longer wavelength (>3.7 μm) mid-infrared light detection. Recently a few b-As$_x$P$_{1-x}$ mid-infrared photodetectors operational up to 8 μm have been demonstrated.[90,91]

3.3. Black Phosphorus Photodetectors and Optical Modulators

Photodetectors are one of the most important components in photonics. Bulk black phosphorus has a bandgap energy of ≈0.33 eV. Therefore, photons with energy larger than that (3.7 μm or shorter in terms of wavelength) can be absorbed by BP through efficient interband transitions, and consequently, be detected. In 2014, the capability of detecting light at visible and near-infrared regions was demonstrated. These detectors had various device configurations based on FET structures (**Figure 5**a, upper left panel),[46,92] local split-gate p–n junction (Figure 5a, upper right panel),[93] BP–molybdenum disulfide (MoS_2) heterojunction p–n junction (Figure 5a, lower left panel),[44] etc. Youngblood et al. fabricated BP photodetector working in the near-infrared telecom band with waveguide-integrated structure to significantly enhance light-BP interaction (Figure 5a, lower right panel).[34] Their detectors worked in the photovoltaic mode and thus reached a speed of 3 GHz. To leverage the optical linear dichroism of black phosphorus, Yuan et al. demonstrated a polarization-sensitive photodetector

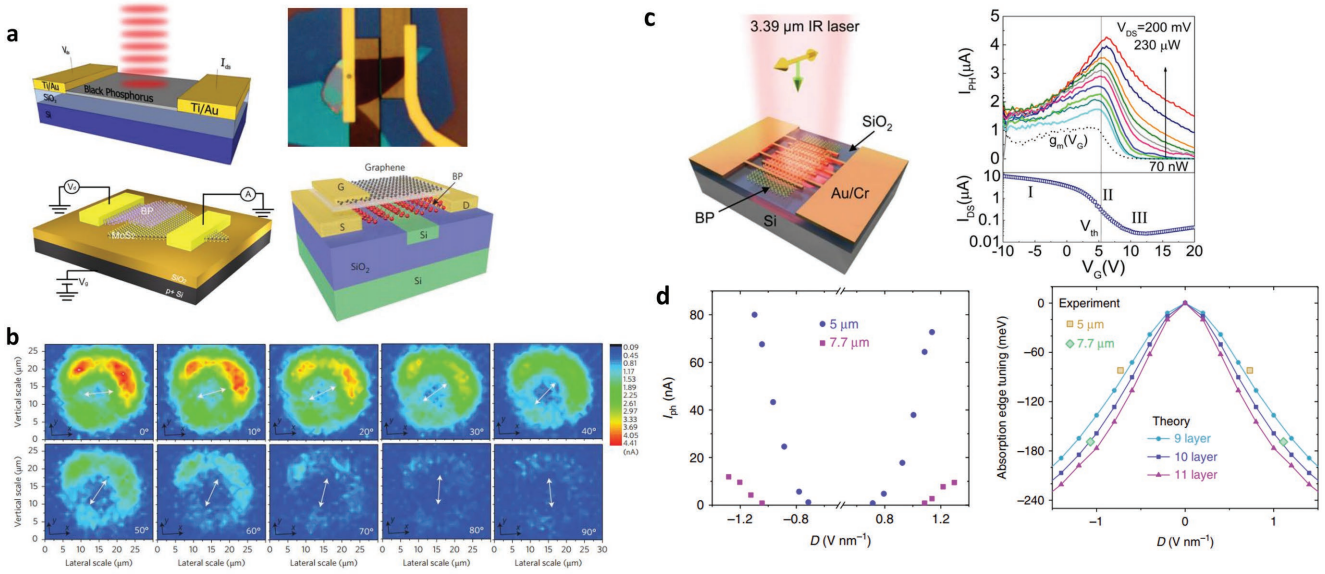

Figure 5. Black phosphorus photodetectors. a) BP photodetectors with varying device configurations. Upper left: FET structure. Adapted with permission.[92] Copyright 2014, American Chemical Society. Upper right: split-gate p–n junction. Adapted with permission.[93] Copyright 2014, Springer Nature. Lower left: BP-MoS_2 p–n junction. Adapted with permission.[44] Copyright 2014, American Chemical Society. Lower right: Si waveguide-integrated detector. Adapted with permission.[34] Copyright 2015, Springer Nature. b) Photocurrent mapping of a BP photodetector (ring-shape) under the illumination light with different polarizations. Adapted with permission.[42] Copyright 2015, Springer Nature. c) Left: Schematic of BP mid-infrared photodetector with interdigitated structure. Right: The device photoresponse under different illumination powers. The photocurrent qualitatively follows the trend of transconductance. Adapted with permission.[94] Copyright 2016, American Chemical Society. d) Left: Photocurrent as a function of vertical displacement field under 5 and 7.7 μm laser illumination respectively. Right: The tuning of BP optical absorption edge as a function of vertical displacement field (Theory). The critical displacement fields where 5 and 7.7 μm photoresponses emerge are denoted (Experiment). Adapted under the terms of the Creative Commons Attribution 4.0 International License.[96] Copyright 2017, Springer Nature.

(Figure 5b).[42] The ratio of the responsivities between the *x*-polarized and *y*-polarized light was enhanced as the wavelength increased, which is also consistent with the symmetry analysis presented above. To make the most of the moderate bandgap of black phosphorus, and to extend the operating spectral range into less-explored but technological important mid-infrared region, Guo et al. constructed interdigitated BP photodetector operating at 3.39 μm with an external responsivity as high as 82 A W^{-1}.[94] The high gain was due to the trapping of one type of photoexcited carriers and thus prolongs the recombination lifetime of the other. The other type of carriers, as a result, has the opportunity to make transit between the source and drain many times before recombination. Their device schematic and the feature of photoresponse are showed in Figure 5c. Because of the decent off-state of BP transistors, their detectors were capable of detecting mid-infrared light at picowatt level. Using time-resolved measurements, Suess et al. revealed the potential of black phosphorus in high-speed mid-infrared optoelectronics up to the band edge energy of 3.7 μm.[95]

Since a moderate vertical electric field significantly reduces the bandgap energy of BP from 300 to below 50 meV, the lower energy photodetection limit of black phosphorus detectors can be further extended. Recently, Chen et al. demonstrated a dual-gate interdigitated photodetector with FET configuration based on h-BN/BP/h-BN-sandwiched heterostructure.[96] As mentioned in the previous section, h-BN encapsulated BP devices show better electrical performance and also improved stability. Their photodetector worked up to 7.7 μm under a vertical electric field, corresponding to photon energy of only 160 meV, much smaller than the BP intrinsic bandgap. The left panel of Figure 5d shows the photocurrent as a function of displacement field for 5 and 7.7 μm laser illumination, respectively. As the field increases, the bandgap shrinks, and the corresponding photocurrent increases. In this case, the intrinsic BP properties were preserved by h-BN encapsulation and the photocurrent generation mechanism was different from the previous reports. The magnitude of photocurrent reached its maximum at charge-neutrality point, which is the key feature of the photoconductive effect. In this regime, excess electrons and holes were generated by the incident photons through interband transition, and were then drifted to the opposite directions under the source–drain bias. In this device, since the active BP layer was well protected by the underneath and top h-BN (the trapping effects were negligible), the intrinsic photoconductive effect could be accessed. This work also provided an alternative evidence of black phosphorus bandgap tunability under an electrical field. In the right panel of Figure 5d, the displacement fields at which 5 and 7.7 μm photoresponses emerge (corresponding to absorption edge decreases of 80 and 170 meV, respectively) are denoted as scatters. They lie within the calculated solid lines. These results are also consistent with the bandgap tuning extracted from the electrical transport study.[35]

Since black arsenic phosphorus has a tunable bandgap as a function of arsenic composition, it may be used to detect long-wave infrared light. Recently, Long et al. and Amani et al. showed that by using b-As_xP_{1-x} with high x value, their detectors worked beyond 3.7 μm with decent responsivities.[90,91] In

both detectors, the lowest photon energy that can be detected is limited by the material bandgap. Interestingly, Viti et al. demonstrated a BP terahertz detector based on plasma-wave rectification effect or thermoelectric effect, depending on the detector working regimes.[97] They later improved their detector performance also by sandwiching a BP layer between two h-BNs layer to preserve the intrinsic properties of BP.[98]

Besides light detection, modulation is also important in photonics. Up to now, the reported black phosphorus optical modulations were mainly based on the two working principles discussed in the "tunable optical properties" section, namely, the Stark effect and the Pauli blocking effect. Stark effect reduces the bandgap under a vertical electric field. Pauli blocking, on the other hand, shifts the absorption edge to higher energy because the increasing doping level blocks the optical transitions at lower energies. Lin et al. theoretically investigated the influence of these two effects on BP optical response and proposed a silicon waveguide-integrated BP optical modulator working in mid-infrared.[39] By the application of a gate voltage, the modulation of BP infrared response was achieved by the interplay of both Stark and Pauli blocking effects, since a gate voltage induced an out-of-plane electric field and also introduced extra doping into the material simultaneously. As a result, both blue shift and red shift of BP absorption edge can happen depending on initial doping, BP thickness, and operational wavelength. **Figure 6**a shows their proposed device structure and the bandgap energy shift as functions of carrier density and BP thickness for the two different mechanisms. Whitney et al. experimentally demonstrated the tunable optical extinction of BP thin films by applying a back-gate bias.[38] However, in their work, the modulation was actually a mixed result of both effects (Figure 6b). To better understand the individual influences of the Stark effect and the Pauli blocking effect on BP optical properties, it is desirable to fabricated dual-gate device where the two gates can control the Fermi level and the electric field penetrates the material separately.[99] In fact, the tunable photocurrent results reported by Chen et al. also probed the optical absorption of black phosphorus purely under an electric field by always examining the photocurrent at charge-neutral point, a condition at which the Fermi level lays in the middle of the tuned bandgap.[96] Although black phosphorus is a promising candidate for mid-infrared modulator applications, its potentials have not been extensively explored. For example, future integration of BP with optical waveguides or cavities can lead to practical modulators operational in a broad mid-infrared wavelength range.

3.4. Black Phosphorus Nonlinear Optics

So far, our discussion focuses on the interaction between black phosphorus and light with relatively low intensity, where linear

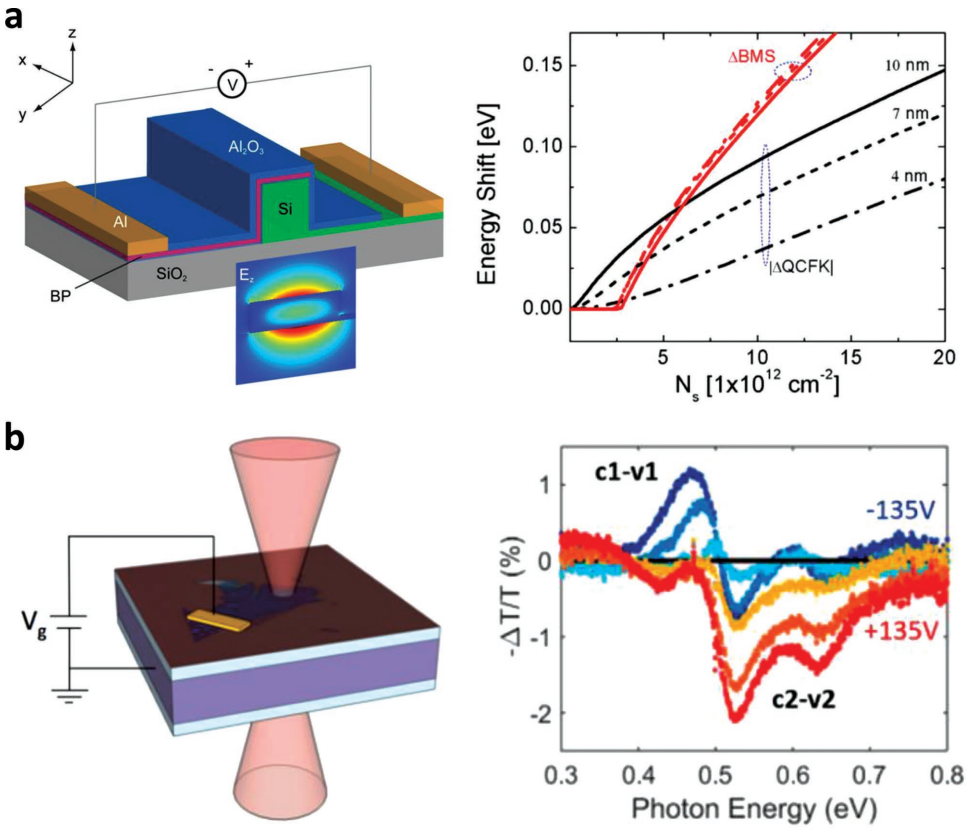

Figure 6. Black phosphorus optical modulators. a) Left: A design of black phosphorus optical modulator based on the structure of Si waveguide. Right: Red (black) lines: Calculated energy shift of bandgap as a function of carrier concentration caused merely by Pauli blocking effect (Stark effect). Adapted with permission.[39] Copyright 2016, American Chemical Society. b) Left: A gate-tunable BP modulator prototype. Right: Relative extinction spectra normalized to zero bias for different gate voltages. Adapted with permission.[38] Copyright 2017, American Chemical Society.

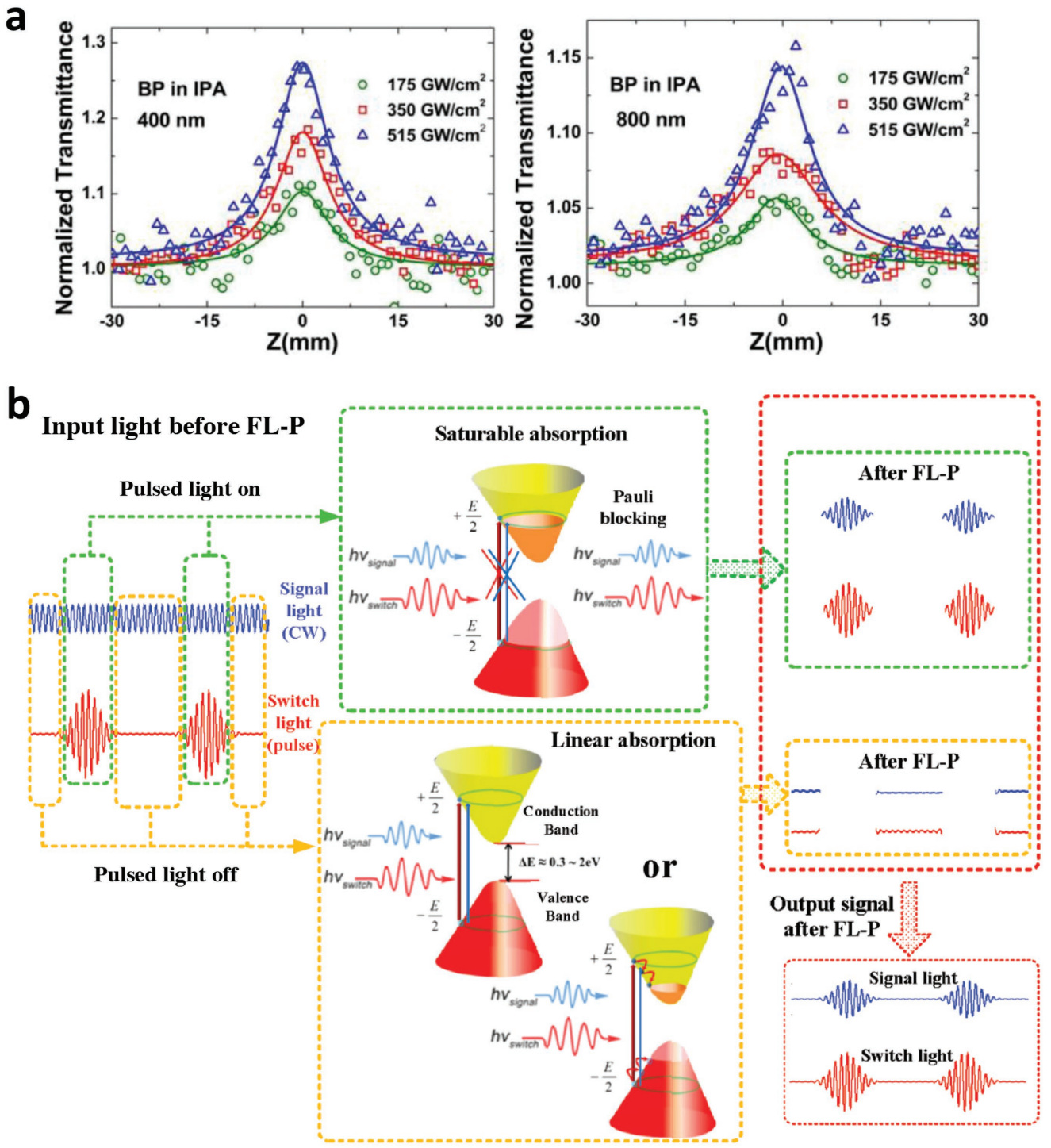

Figure 7. Black phosphorus nonlinear optics. a) Z-scan measurements of BP nanoplatelet dispersions under 400 nm (left) and 800 nm (right) illumination, respectively. Adapted under the terms of the Creative Commons Attribution 4.0 International License.[100] Copyright 2015, Optical Society of America. b) Schematic of the all-optical modulator based on BP saturable absorber. A continuous-wave signal and a control light pulse are coupled into few-layer black phosphorus (FL-P) simultaneously. When the pulsed light is on, it saturates the BP absorption so that the transmittance of the continuous signal light is high. When the pulsed light is off, the FL-P absorbs the signal light strongly such that it is significantly attenuated. Therefore, the output signal after FL-P is efficiently modulated by the pulsed control light. Adapted with permission.[106] Copyright 2017, Wiley-VCH.

optical response dominates. The nonlinear optical properties of BP are equally impressive.[48,100–103] Lu et al. demonstrated saturable light absorption in liquid exfoliated black phosphorus.[100] **Figure 7**a shows their results of *Z*-scan measurements on BP nanoplatelets dispersed in isopropyl alcohol. In the figure, the $Z = 0$ position corresponds to the focus point where the

incident light intensity is maximized. The normalized transmittance increases as the BP sample moves toward the focus point, indicating the light absorbed by BP nanoplatelets gradually saturated. Also, the increasing power noted in the legends causes increasing transmittance, which is also consistent with the saturable absorption behaviors. They also revealed the broadband nonlinear optical response from visible (400 nm) to mid-infrared (1930 nm), showing the great potentials of BP in the field of nonlinear optics across a broad wavelength range.

Using the pump–probe method, Wang et al. investigated the ultrafast carrier dynamics in black phosphorus.[104] The nonlinear optical measurements show that BP is a promising saturable absorber in near-infrared and mid-infrared, due to the fast relaxation of excited carriers. Chen et al. demonstrated the applications of BP in Q-switch and mode-locked lasers by placing mechanical exfoliated BP into an erbium-doped fiber laser cavity.[48] The nonlinear properties of BP also make it suitable for all-optical signal processing. Zheng et al. demonstrated an optical Kerr switch and a four-wave-mixing-based wavelength converter based on BP.[105] Their use of metal-ion-modified black phosphorus was also proven to be effective against oxidation. The same research group has also fabricated an all-optical thresholder, in which the transmittance of light is possible only when the light intensity reaches certain threshold.[106] The device also worked based on the principle that the high-intensity light saturates the absorption of BP. Moreover, an all-optical modulator was demonstrated.[106] In this device, a continuous-wave signal and a control light pulse are focused on the device simultaneously. The intensity of the light pulse was high such that it saturates the BP absorption. The continuous signal light can have high transmittance when the pulsed light is on, but is significantly attenuated when the pulsed light is off. As a result, efficient optical modulation of the signal light is realized using the pulsed control light. The device working principles are shown schematically in Figure 7b. Besides black phosphorus flakes, ultrasmall black phosphorus quantum dots were reported as well with desirable nonlinear optical properties.[107]

3.5. Black Phosphorus Biophotonics

Phosphorus is an essential element for organisms, and it makes up ≈1% of the weight in a human body.[108] Therefore, black phosphorus has inherent biocompatibility, biodegradability, and nontoxicity for human body.[109–111] Together with the BP's strong optical response in infrared, these desirable properties make it promising for biophotonic and clinical applications.

Sun et al. used black phosphorus quantum dots as photothermal agents for cancer photothermal therapy.[109] In short, BP quantum dots were first prepared by a liquid exfoliation method, and near-infrared light was used to induce temperature increase in BP quantum dots. Due to the decent photothermal conversion efficiency of the as-prepared BP agent, the infrared light induces strong heating effect to treat the cancer cells. Their experiments also showed that the BP agent was not toxic to different types of cells. Shao et al. used poly (lactic-co-glycolic acid) (PLGA) loaded BP quantum dots for photothermal therapy.[110] In their work, the degradation of BP in the presence of oxygen and water actually became an intrinsic advantage, since it made the agent more biodegradable in human body. The coated PLGA protected the core of BP quantum dots while also controlled the degradation rate. The authors performed both in vitro and in vivo experiments to confirm its nontoxicity and biocompatibility. In another work, Qiu et al. showed that by loading BP nanostructure and therapeutic drug into a hydrogel, it was possible to accurately control the drug release rate by adjusting near-infrared radiation conditions.[111] In this case, black phosphorus absorbed the near-infrared light and efficiently converted it into heat, and the heat was used to hydrolyze and soften the hydrogel. Therefore, the drug could be controllably released into the environment.[111]

4. Outlook

In this article, we have reviewed the latest progress on a few important research topics of black phosphorus photonics. Black phosphorus may enable various photonic applications in the infrared wavelength range, which cannot be easily accessed by other 2D materials. Looking forward, probably the biggest challenge is its wafer scale synthesis. At current stage, black phosphorus thin films are mostly obtained by exfoliation methods, including mechanical and liquid exfoliation.[3–6,112–114] A controllable large-scale synthesis approach of BP thin films is increasingly expected. The high pressure (≈10 GPa) red phosphorus to black phosphorus conversion by phase transition approach reported by Li et al. shows a possible route toward wafer-scale synthesis (**Figure 8**a, top panel).[57] However, they only utilized high pressure and the effect of temperature was not explored. Moreover, high temperature is a favorable condition in crystal formation process, since it enlarges the grain size.[115] Very recently, Li et al. realized the synthesis of highly crystalline BP thin film on sapphire at an elevated temperature of 700 °C and a reduced pressure of 1.5 GPa.[58] The as-grown BP showed much larger domain size and much improved carrier mobility. Moreover, they demonstrated that for red phosphorus covered by exfoliated h-BN, the converted h-BN/BP heterostructure had atomically sharp interface and the layered structure was clearly seen (Figure 8a, middle panel). Another approach with similar red phosphorus predeposition method used in situ chemical vapor reaction with the presence of mineralizing agents (tin and tin (IV) iodide), and the synthesis of BP thin-film flakes directly on silicon substrate was realized (Figure 8a, bottom panel).[59] However, in this method, the synthesized BP films were not continuous. Further optimizations are needed to address this issue.

Moreover, another clear challenge is that bare black phosphorus is unstable in ambient condition.[7,51] Over the last years, different groups have developed a few effective approaches to improve its stability, including chemical modification,[52,116] polymer coating,[117] atomic layer deposition (e.g., Al_2O_3, HfO_2) coating,[118] metal ion modification,[54] fluorine atom adsorption,[55] graphene oxide/BP aerogel,[56] encapsulation using other inert 2D material (e.g., h-BN, graphene),[53] etc. Among them, h-BN/BP/h-BN heterostructure is very promising for future electronics and optoelectronics, since large-area multilayer h-BN for high-quality dielectric has already been realized,[119] and h-BN coverage preserves the intrinsic quality

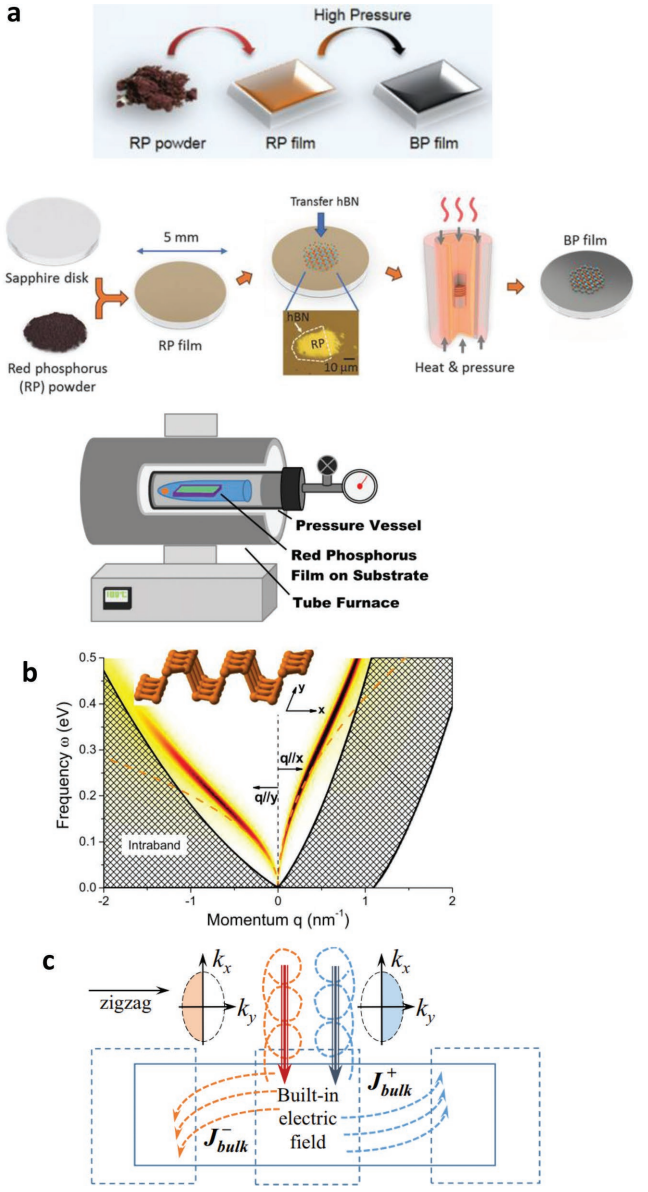

Figure 8. Wafer-scale synthesis and future work. a) Top: Synthesis of thin-film black phosphorus by the high pressure approach. First, red phosphorus thin film is thermally deposited to a flexible substrate from red phosphorus powder. Then, high pressure is applied to convert red phosphorus to BP by phase transition. Adapted with permission.[57] Copyright 2015, IOP Publishing. Middle: Synthesis of highly crystalline BP thin film and the formation of h-BN/BP heterostructure at elevated temperature. Adapted with permission.[58] Copyright 2018, Wiley-VCH. Bottom: In situ synthesis of black phosphorus film directly on silicon substrate. The red phosphorus film was predeposited on the substrate. The chemical reactions take place with the assistance of the mineralizing agents. Adapted with permission.[59] Copyright 2016, IOP Publishing. b) Calculated energy loss function and plasmon dispersion for monolayer BP along the two main crystal directions. Adapted with permission.[120] Copyright 2014, American Physical Society. c) The interaction between circularly polarized light and symmetry broken BP. Left and right circularly polarized lights couple to the electronic states with Berry curvatures of different polarities, leading to the opposite topological currents. The Berry curvature mapping in *k*-space is distinct from those in 2D hexagonal lattice systems. Adapted with permission.[121] Copyright 2015, American Physical Society.

of BP. We also want to emphasize that the degradation of bare BP is not necessarily an undesirable property. In fact, its biodegradability and biocompatibility make it a novel material for biophotonic applications.

Besides optical detection and modulation, black phosphorus may also play a role in infrared light sources. As mentioned above, strong photoluminescence has been observed in monolayer and few-layer BP.[71,72] It may be possible to develop tunable electroluminescence light source based on BP, leveraging its tunable bandgap. Moreover, the collective carrier excitation (plasmon) in black phosphorus has yet to be experimentally revealed, although it was predicted theoretically. Interestingly, the plasmon modes in BP are predicted to be highly anisotropic and in armchair direction, the mode is long-lived up to near infrared (Figure 8b).[120] The fast carrier dynamics and decent saturable absorption over the broad infrared spectrum make it promising for applications such as laser mode-locker, ultrafast optical modulator and switch, wavelength converter, all-optical signal processing, etc.[48,105,106]

Recently, Low et al. theoretically studied the valley current in symmetry broken black phosphorus thin films.[121] Conventional valley physics has been extensively investigated in 2D hexagonal lattice systems, like TMDCs and graphene.[122–128] In black phosphorus, however, due to the different band structure, the properties of topological valley current were predicted to be distinctively different.[121] It may be possible to observe finite transverse Hall voltage directly under a longitudinal drive current, even without circularly polarized light excitation.[121] This was not possible in TMDCs or graphene. Therefore, the new effects of coupling between BP and circularly polarized light can also be interesting. Figure 8c shows that, in the symmetry broken regime, right or left circularly polarized light couples to states with Berry curvature of a certain polarity. As a result, this will generate finite topological current with components along both the longitudinal and transverse directions.

In summary, during the past few years, black phosphorus has attracted significant attention due to many exciting properties such as its strong interaction with infrared light, high carrier mobility, desirable and widely tunable bandgap, and the interesting in-plane anisotropy. Numerous proof-of-concept devices such as transistors, photodetectors, and optical modulators were demonstrated with superior performances. Among these, near-infrared and mid-infrared photonics is especially promising, since black phosphorus largely outperforms other 2D material counterparts within this wavelength range. Future efforts on wafer-scale synthesis and device developments may ultimately lead to its deployment in various infrared applications especially in the mid-infrared wavelength ranging from 2 to 8 μm.

Acknowledgements

The black phosphorus photonic work at Yale is primarily supported by the National Science Foundation EFRI-2DARE program. F.X. also acknowledges the partial support by the Office of Naval Research Young Investigator Program (ONR-YIP). A.C.-G. acknowledges funding from the European Research Council (ERC) under the European Union's Horizon 2020 research and innovation programme (grant agreement no. 755655, ERC-StG 2017 project 2D-TOPSENSE). R.F. thanks the

Netherlands Organisation for Scientific Research (NWO) for support through a Rubicon grant. This review is part of the *Advanced Optical Materials* Hall of Fame article series, which recognizes the excellent contributions of leading researchers to the field of optical materials science.

Conflict of Interest

The authors declare no conflict of interest.

Keywords

bandgap engineering, black phosphorus, linear dichroism, optoelectronic devices, photonics

Received: March 20, 2018
Revised: May 28, 2018
Published online: July 25, 2018

[1] P. W. Bridgman, *J. Am. Chem. Soc.* **1914**, *36*, 1344.
[2] A. Morita, *Appl. Phys. A* **1986**, *39*, 227.
[3] L. Li, Y. Yu, G. J. Ye, Q. Ge, X. Ou, H. Wu, D. Feng, X. H. Chen, Y. Zhang, *Nat. Nanotechnol.* **2014**, *9*, 372.
[4] H. Liu, A. T. Neal, Z. Zhu, Z. Luo, X. Xu, D. Tománek, P. D. Ye, *ACS Nano* **2014**, *8*, 4033.
[5] F. Xia, H. Wang, Y. Jia, *Nat. Commun.* **2014**, *5*, 4458.
[6] S. P. Koenig, R. A. Doganov, H. Schmidt, A. H. Castro Neto, B. Özyilmaz, *Appl. Phys. Lett.* **2014**, *104*, 103106.
[7] A. Castellanos-Gomez, L. Vicarelli, E. Prada, J. O. Island, K. L. Narasimha-Acharya, S. I. Blanter, D. J. Groenendijk, M. Buscema, G. A. Steele, J. V. Alvarez, H. W. Zandbergen, J. J. Palacios, H. S. J. van der Zant, *2D Mater.* **2014**, *1*, 025001.
[8] J. Qiao, X. Kong, Z.-X. Hu, F. Yang, W. Ji, *Nat. Commun.* **2014**, *5*, 4475.
[9] V. Tran, R. Soklaski, Y. Liang, L. Yang, *Phys. Rev. B* **2014**, *89*, 235319.
[10] X. Ling, H. Wang, S. Huang, F. Xia, M. S. Dresselhaus, *Proc. Natl. Acad. Sci. USA* **2015**, *112*, 4523.
[11] H. Liu, Y. Du, Y. Deng, P. D. Ye, *Chem. Soc. Rev.* **2015**, *44*, 2732.
[12] S. C. Dhanabalan, J. S. Ponraj, Z. Guo, S. Li, Q. Bao, H. Zhang, *Adv. Sci.* **2017**, *4*, 1600305.
[13] Y. Zhou, M. Zhang, Z. Guo, L. Miao, S.-T. Han, Z. Wang, X. Zhang, H. Zhang, Z. Peng, *Mater. Horiz.* **2017**, *4*, 997.
[14] X. Wang, S. Lan, *Adv. Opt. Photonics* **2016**, *8*, 618.
[15] F. Xia, H. Wang, D. Xiao, M. Dubey, A. Ramasubramaniam, *Nat. Photonics* **2014**, *8*, 899.
[16] K. S. Novoselov, A. K. Geim, S. V. Morozov, D. Jiang, M. I. Katsnelson, I. V. Grigorieva, S. V. Dubonos, A. A. Firsov, *Nature* **2005**, *438*, 197.
[17] Y. Zhang, Y.-W. Tan, H. L. Stormer, P. Kim, *Nature* **2005**, *438*, 201.
[18] F. Schwierz, *Nat. Nanotechnol.* **2010**, *5*, 487.
[19] K. S. Novoselov, A. K. Geim, S. V. Morozov, D. Jiang, Y. Zhang, S. V. Dubonos, I. V. Grigorieva, A. A. Firsov, *Science* **2004**, *306*, 666.
[20] R. R. Nair, P. Blake, A. N. Grigorenko, K. S. Novoselov, T. J. Booth, T. Stauber, N. M. R. Peres, A. K. Geim, *Science* **2008**, *320*, 1308.
[21] X. Gan, K. F. Mak, Y. Gao, Y. You, F. Hatami, J. Hone, T. F. Heinz, D. Englund, *Nano Lett.* **2012**, *12*, 5626.
[22] T. Low, P. Avouris, *ACS Nano* **2014**, *8*, 1086.
[23] F. Xia, T. Mueller, Y.-m. Lin, A. Valdes-Garcia, P. Avouris, *Nat. Nanotechnol.* **2009**, *4*, 839.
[24] T. Mueller, F. Xia, P. Avouris, *Nat. Photonics* **2010**, *4*, 297.
[25] X. Gan, R.-J. Shiue, Y. Gao, I. Meric, T. F. Heinz, K. Shepard, J. Hone, S. Assefa, D. Englund, *Nat. Photonics* **2013**, *7*, 883.
[26] X. Wang, Z. Cheng, K. Xu, H. K. Tsang, J.-B. Xu, *Nat. Photonics* **2013**, *7*, 888.
[27] A. Pospischil, M. Humer, M. M. Furchi, D. Bachmann, R. Guider, T. Fromherz, T. Mueller, *Nat. Photonics* **2013**, *7*, 892.
[28] Q. H. Wang, K. Kalantar-Zadeh, A. Kis, J. N. Coleman, M. S. Strano, *Nat. Nanotechnol.* **2012**, *7*, 699.
[29] K. F. Mak, C. Lee, J. Hone, J. Shan, T. F. Heinz, *Phys. Rev. Lett.* **2010**, *105*, 136805.
[30] A. Splendiani, L. Sun, Y. Zhang, T. Li, J. Kim, C.-Y. Chim, G. Galli, F. Wang, *Nano Lett.* **2010**, *10*, 1271.
[31] K. Watanabe, T. Taniguchi, H. Kanda, *Nat. Mater.* **2004**, *3*, 404.
[32] J. H. Davies, *The Physics of Low-dimensional Semiconductors: An Introduction*, Cambridge University Press, New York, New York, USA **1997**.
[33] M. Fox, *Optical Properties of Solids*, OUP, Oxford **2010**.
[34] N. Youngblood, C. Chen, S. J. Koester, M. Li, *Nat. Photonics* **2015**, *9*, 247.
[35] B. Deng, V. Tran, Y. Xie, H. Jiang, C. Li, Q. Guo, X. Wang, H. Tian, S. J. Koester, H. Wang, J. J. Cha, Q. Xia, L. Yang, F. Xia, *Nat. Commun.* **2017**, *8*, 14474.
[36] Y. Liu, Z. Qiu, A. Carvalho, Y. Bao, H. Xu, S. J. R. Tan, W. Liu, A. H. Castro Neto, K. P. Loh, J. Lu, *Nano Lett.* **2017**, *17*, 1970.
[37] R. Roldán, A. Castellanos-Gomez, *Nat. Photonics* **2017**, *11*, 407.
[38] W. S. Whitney, M. C. Sherrott, D. Jariwala, W.-H. Lin, H. A. Bechtel, G. R. Rossman, H. A. Atwater, *Nano Lett.* **2017**, *17*, 78.
[39] C. Lin, R. Grassi, T. Low, A. S. Helmy, *Nano Lett.* **2016**, *16*, 1683.
[40] D. Li, J.-R. Xu, K. Ba, N. Xuan, M. Chen, Z. Sun, Y.-Z. Zhang, Z. Zhang, *2D Mater.* **2017**, *4*, 031009.
[41] S.-L. Yan, Z.-J. Xie, J.-H. Chen, T. Taniguchi, K. Watanabe, *Chin. Phys. Lett.* **2017**, *34*, 047304.
[42] H. Yuan, X. Liu, F. Afshinmanesh, W. Li, G. Xu, J. Sun, B. Lian, A. G. Curto, G. Ye, Y. Hikita, Z. Shen, S.-C. Zhang, X. Chen, M. Brongersma, H. Y. Hwang, Y. Cui, *Nat. Nanotechnol.* **2015**, *10*, 707.
[43] H. Wang, X. Wang, F. Xia, L. Wang, H. Jiang, Q. Xia, M. L. Chin, M. Dubey, S.-J. Han, *Nano Lett.* **2014**, *14*, 6424.
[44] Y. Deng, Z. Luo, N. J. Conrad, H. Liu, Y. Gong, S. Najmaei, P. M. Ajayan, J. Lou, X. Xu, P. D. Ye, *ACS Nano* **2014**, *8*, 8292.
[45] W. Zhu, M. N. Yogeesh, S. Yang, S. H. Aldave, J.-S. Kim, S. Sonde, L. Tao, N. Lu, D. Akinwande, *Nano Lett.* **2015**, *15*, 1883.
[46] M. Engel, M. Steiner, P. Avouris, *Nano Lett.* **2014**, *14*, 6414.
[47] A. N. Abbas, B. Liu, L. Chen, Y. Ma, S. Cong, N. Aroonyadet, M. Köpf, T. Nilges, C. Zhou, *ACS Nano* **2015**, *9*, 5618.
[48] Y. Chen, G. Jiang, S. Chen, Z. Guo, X. Yu, C. Zhao, H. Zhang, Q. Bao, S. Wen, D. Tang, D. Fan, *Opt. Express* **2015**, *23*, 12823.
[49] X. Zhang, H. Xie, Z. Liu, C. Tan, Z. Luo, H. Li, J. Lin, L. Sun, W. Chen, Z. Xu, L. Xie, W. Huang, H. Zhang, *Angew. Chem., Int. Ed.* **2015**, *54*, 3653.
[50] H. Tian, Q. Guo, Y. Xie, H. Zhao, C. Li, J. J. Cha, F. Xia, H. Wang, *Adv. Mater.* **2016**, *28*, 4991.
[51] J. O. Island, G. A. Steele, H. S. J. van der Zant, A. Castellanos-Gomez, *2D Mater.* **2015**, *2*, 011002.
[52] C. R. Ryder, J. D. Wood, S. A. Wells, Y. Yang, D. Jariwala, T. J. Marks, G. C. Schatz, M. C. Hersam, *Nat. Chem.* **2016**, *8*, 597.
[53] R. A. Doganov, E. C. T. O'Farrell, S. P. Koenig, Y. Yeo, A. Ziletti, A. Carvalho, D. K. Campbell, D. F. Coker, K. Watanabe, T. Taniguchi, A. H. Castro Neto, B. Özyilmaz, *Nat. Commun.* **2015**, *6*, 6647.
[54] Z. Guo, S. Chen, Z. Wang, Z. Yang, F. Liu, Y. Xu, J. Wang, Y. Yi, H. Zhang, L. Liao, P. K. Chu, X. F. Yu, *Adv. Mater.* **2017**, *29*, 1703811.

[55] X. Tang, W. Liang, J. Zhao, Z. Li, M. Qiu, T. Fan, C. S. Luo, Y. Zhou, Y. Li, Z. Guo, D. Fan, H. Zhang, *Small* **2017**, *13*, 1702739.
[56] C. Xing, G. Jing, X. Liang, M. Qiu, Z. Li, R. Cao, X. Li, D. Fan, H. Zhang, *Nanoscale* **2017**, *9*, 8096.
[57] X. Li, B. Deng, X. Wang, S. Chen, M. Vaisman, S.-i. Karato, G. Pan, M. L. Lee, J. Cha, H. Wang, F. Xia, *2D Mater.* **2015**, *2*, 031002.
[58] C. Li, Y. Wu, B. Deng, Y. Xie, Q. Guo, S. Yuan, X. Chen, M. Bhuiyan, Z. Wu, K. Watanabe, T. Taniguchi, H. Wang, J. J. Cha, M. Snure, Y. Fei, F. Xia, *Adv. Mater.* **2018**, *30*, 1703748.
[59] J. B. Smith, D. Hagaman, H.-F. Ji, *Nanotechnology* **2016**, *27*, 215602.
[60] S. Dong, A. Zhang, K. Liu, J. Ji, Y. G. Ye, X. G. Luo, X. H. Chen, X. Ma, Y. Jie, C. Chen, X. Wang, Q. Zhang, *Phys. Rev. Lett.* **2016**, *116*, 087401.
[61] W. Zhu, S. Park, M. N. Yogeesh, K. M. McNicholas, S. R. Bank, D. Akinwande, *Nano Lett.* **2016**, *16*, 2301.
[62] L. Li, G. J. Ye, V. Tran, R. Fei, G. Chen, H. Wang, J. Wang, K. Watanabe, T. Taniguchi, L. Yang, X. H. Chen, Y. Zhang, *Nat. Nanotechnol.* **2015**, *10*, 608.
[63] N. Gillgren, D. Wickramaratne, Y. Shi, T. Espiritu, J. Yang, J. Hu, J. Wei, X. Liu, Z. Mao, K. Watanabe, T. Taniguchi, M. Bockrath, Y. Barlas, R. K. Lake, C. N. Lau, *2D Mater.* **2015**, *2*, 011001.
[64] X. Chen, Y. Wu, Z. Wu, Y. Han, S. Xu, L. Wang, W. Ye, T. Han, Y. He, Y. Cai, N. Wang, *Nat. Commun.* **2015**, *6*, 7315.
[65] L. Li, F. Yang, G. J. Ye, Z. Zhang, Z. Zhu, W. Lou, X. Zhou, L. Li, K. Watanabe, T. Taniguchi, K. Chang, Y. Wang, X. H. Chen, Y. Zhang, *Nat. Nanotechnol.* **2016**, *11*, 593.
[66] C. R. Dean, A. F. Young, I. Meric, C. Lee, L. Wang, S. Sorgenfrei, K. Watanabe, T. Taniguchi, P. Kim, K. L. Shepard, J. Hone, *Nat. Nanotechnol.* **2010**, *5*, 722.
[67] L. Wang, I. Meric, P. Y. Huang, Q. Gao, Y. Gao, H. Tran, T. Taniguchi, K. Watanabe, L. M. Campos, D. A. Muller, J. Guo, P. Kim, J. Hone, K. L. Shepard, C. R. Dean, *Science* **2013**, *342*, 614.
[68] G. Long, D. Maryenko, J. Shen, S. Xu, J. Hou, Z. Wu, W. K. Wong, T. Han, J. Lin, Y. Cai, R. Lortz, N. Wang, *Nano Lett.* **2016**, *16*, 7768.
[69] N. Mao, J. Tang, L. Xie, J. Wu, B. Han, J. Lin, S. Deng, W. Ji, H. Xu, K. Liu, L. Tong, J. Zhang, *J. Am. Chem. Soc.* **2016**, *138*, 300.
[70] J. Quereda, P. San-Jose, V. Parente, L. Vaquero-Garzon, A. J. Molina-Mendoza, N. Agraït, G. Rubio-Bollinger, F. Guinea, R. Roldán, A. Castellanos-Gomez, *Nano Lett.* **2016**, *16*, 2931.
[71] X. Wang, A. M. Jones, K. L. Seyler, V. Tran, Y. Jia, H. Zhao, H. Wang, L. Yang, X. Xu, F. Xia, *Nat. Nanotechnol.* **2015**, *10*, 517.
[72] L. Li, J. Kim, C. Jin, G. J. Ye, D. Y. Qiu, F. H. da Jornada, Z. Shi, L. Chen, Z. Zhang, F. Yang, K. Watanabe, T. Taniguchi, W. Ren, S. G. Louie, X. H. Chen, Y. Zhang, F. Wang, *Nat. Nanotechnol.* **2016**, *12*, 21.
[73] G. Zhang, S. Huang, A. Chaves, C. Song, V. O. Özçelik, T. Low, H. Yan, *Nat. Commun.* **2017**, *8*, 14071.
[74] T. Low, A. S. Rodin, A. Carvalho, Y. Jiang, H. Wang, F. Xia, A. H. Castro Neto, *Phys. Rev. B* **2014**, *90*, 075434.
[75] H.-C. Chung, C.-P. Chang, C.-Y. Lin, M.-F. Lin, *Phys. Chem. Chem. Phys.* **2016**, *18*, 7573.
[76] C. D. Spataru, S. Ismail-Beigi, L. X. Benedict, S. G. Louie, *Phys. Rev. Lett.* **2004**, *92*, 077402.
[77] Q. Bao, H. Zhang, Y. Wang, Z. Ni, Y. Yan, Z. X. Shen, K. P. Loh, D. Y. Tang, *Adv. Funct. Mater.* **2009**, *19*, 3077.
[78] A. N. Grigorenko, M. Polini, K. S. Novoselov, *Nat. Photonics* **2012**, *6*, 749.
[79] K. F. Mak, L. Ju, F. Wang, T. F. Heinz, *Solid State Commun.* **2012**, *152*, 1341.
[80] H. Yan, F. Xia, W. Zhu, M. Freitag, C. Dimitrakopoulos, A. A. Bol, G. Tulevski, P. Avouris, *ACS Nano* **2011**, *5*, 9854.
[81] S. L. Chuang, *Physics of Photonic Devices*, John Wiley & Sons, Hoboken, New Jersey, USA **2009**.
[82] D. A. B. Miller, D. S. Chemla, T. C. Damen, A. C. Gossard, W. Wiegmann, T. H. Wood, C. A. Burrus, *Phys. Rev. Lett.* **1984**, *53*, 2173.
[83] J. Kim, S. S. Baik, S. H. Ryu, Y. Sohn, S. Park, B.-G. Park, J. Denlinger, Y. Yi, H. J. Choi, K. S. Kim, *Science* **2015**, *349*, 723.
[84] Z. J. Xiang, G. J. Ye, C. Shang, B. Lei, N. Z. Wang, K. S. Yang, D. Y. Liu, F. B. Meng, X. G. Luo, L. J. Zou, Z. Sun, Y. Zhang, X. H. Chen, *Phys. Rev. Lett.* **2015**, *115*, 186403.
[85] J. Guo, H. Wang, F. von Rohr, W. Yi, Y. Zhou, Z. Wang, S. Cai, S. Zhang, X. Li, Y. Li, J. Liu, K. Yang, A. Li, S. Jiang, Q. Wu, T. Xiang, R. J. Cava, L. Sun, *Phys. Rev. B* **2017**, *96*, 224513.
[86] J. A. Flores-Livas, A. Sanna, A. P. Drozdov, L. Boeri, G. Profeta, M. Eremets, S. Goedecker, *Phys. Rev. Mater.* **2017**, *1*, 024802.
[87] A. S. Rodin, A. Carvalho, A. H. Castro Neto, *Phys. Rev. Lett.* **2014**, *112*, 176801.
[88] P.-L. Gong, D.-Y. Liu, K.-S. Yang, Z.-J. Xiang, X.-H. Chen, Z. Zeng, S.-Q. Shen, L.-J. Zou, *Phys. Rev. B* **2016**, *93*, 195434.
[89] B. Liu, M. Köpf, A. N. Abbas, X. Wang, Q. Guo, Y. Jia, F. Xia, R. Weihrich, F. Bachhuber, F. Pielnhofer, H. Wang, R. Dhall, S. B. Cronin, M. Ge, X. Fang, T. Nilges, C. Zhou, *Adv. Mater.* **2015**, *27*, 4423.
[90] M. Long, A. Gao, P. Wang, H. Xia, C. Ott, C. Pan, Y. Fu, E. Liu, X. Chen, W. Lu, T. Nilges, J. Xu, X. Wang, W. Hu, F. Miao, *Sci. Adv.* **2017**, *3*, e1700589.
[91] M. Amani, E. Regan, J. Bullock, G. H. Ahn, A. Javey, *ACS Nano* **2017**, *11*, 11724.
[92] M. Buscema, D. J. Groenendijk, S. I. Blanter, G. A. Steele, H. S. J. van der Zant, A. Castellanos-Gomez, *Nano Lett.* **2014**, *14*, 3347.
[93] M. Buscema, D. J. Groenendijk, G. A. Steele, H. S. J. van der Zant, A. Castellanos-Gomez, *Nat. Commun.* **2014**, *5*, 4651.
[94] Q. Guo, A. Pospischil, M. Bhuiyan, H. Jiang, H. Tian, D. Farmer, B. Deng, C. Li, S.-J. Han, H. Wang, Q. Xia, T.-P. Ma, T. Mueller, F. Xia, *Nano Lett.* **2016**, *16*, 4648.
[95] R. J. Suess, E. Leong, J. L. Garrett, T. Zhou, R. Salem, J. N. Munday, T. E. Murphy, M. Mittendorff, *2D Mater.* **2016**, *3*, 041006.
[96] X. Chen, X. Lu, B. Deng, O. Sinai, Y. Shao, C. Li, S. Yuan, V. Tran, K. Watanabe, T. Taniguchi, D. Naveh, L. Yang, F. Xia, *Nat. Commun.* **2017**, *8*, 1672.
[97] L. Viti, J. Hu, D. Coquillat, W. Knap, A. Tredicucci, A. Politano, M. S. Vitiello, *Adv. Mater.* **2015**, *27*, 5567.
[98] L. Viti, J. Hu, D. Coquillat, A. Politano, C. Consejo, W. Knap, M. S. Vitiello, *Adv. Mater.* **2016**, *28*, 7390.
[99] Y. Zhang, T.-T. Tang, C. Girit, Z. Hao, M. C. Martin, A. Zettl, M. F. Crommie, Y. R. Shen, F. Wang, *Nature* **2009**, *459*, 820.
[100] S. B. Lu, L. L. Miao, Z. N. Guo, X. Qi, C. J. Zhao, H. Zhang, S. C. Wen, D. Y. Tang, D. Y. Fan, *Opt. Express* **2015**, *23*, 11183.
[101] Z.-C. Luo, M. Liu, Z.-N. Guo, X.-F. Jiang, A.-P. Luo, C.-J. Zhao, X.-F. Yu, W.-C. Xu, H. Zhang, *Opt. Express* **2015**, *23*, 20030.
[102] D. Li, H. Jussila, L. Karvonen, G. Ye, H. Lipsanen, X. Chen, Z. Sun, *Sci. Rep.* **2015**, *5*, 15899.
[103] J. Sotor, G. Sobon, W. Macherzynski, P. Paletko, K. M. Abramski, *Appl. Phys. Lett.* **2015**, *107*, 051108.
[104] K. Wang, B. M. Szydłowska, G. Wang, X. Zhang, J. J. Wang, J. J. Magan, L. Zhang, J. N. Coleman, J. Wang, W. J. Blau, *ACS Nano* **2016**, *10*, 6923.
[105] J. Zheng, Z. Yang, C. Si, Z. Liang, X. Chen, R. Cao, Z. Guo, K. Wang, Y. Zhang, J. Ji, M. Zhang, D. Fan, H. Zhang, *ACS Photonics* **2017**, *4*, 1466.
[106] J. Zheng, X. Tang, Z. Yang, Z. Liang, Y. Chen, K. Wang, Y. Song, Y. Zhang, J. Ji, Y. Liu, D. Fan, H. Zhang, *Adv. Opt. Mater.* **2017**, *5*, 1700026.

[107] Y. Xu, Z. Wang, Z. Guo, H. Huang, Q. Xiao, H. Zhang, X. F. Yu, *Adv. Opt. Mater.* **2016**, *4*, 1223.
[108] D. L. Childers, J. Corman, M. Edwards, J. J. Elser, *BioScience* **2011**, *61*, 117.
[109] Z. Sun, H. Xie, S. Tang, X. F. Yu, Z. Guo, J. Shao, H. Zhang, H. Huang, H. Wang, P. K. Chu, *Angew. Chem., Int. Ed.* **2015**, *54*, 11526.
[110] J. Shao, H. Xie, H. Huang, Z. Li, Z. Sun, Y. Xu, Q. Xiao, X.-F. Yu, Y. Zhao, H. Zhang, H. Wang, P. K. Chu, *Nat. Commun.* **2016**, *7*, 12967.
[111] M. Qiu, D. Wang, W. Liang, L. Liu, Y. Zhang, X. Chen, D. K. Sang, C. Xing, Z. Li, B. Dong, F. Xing, D. Fan, S. Bao, H. Zhang, Y. Cao, *Proc. Natl. Acad. Sci. USA* **2018**, *115*, 501.
[112] J. R. Brent, N. Savjani, E. A. Lewis, S. J. Haigh, D. J. Lewis, P. O'Brien, *Chem. Commun.* **2014**, *50*, 13338.
[113] P. Yasaei, B. Kumar, T. Foroozan, C. Wang, M. Asadi, D. Tuschel, J. E. Indacochea, R. F. Klie, A. Salehi-Khojin, *Adv. Mater.* **2015**, *27*, 1887.
[114] D. Hanlon, C. Backes, E. Doherty, C. S. Cucinotta, N. C. Berner, C. Boland, K. Lee, A. Harvey, P. Lynch, Z. Gholamvand, S. Zhang, K. Wang, G. Moynihan, A. Pokle, Q. M. Ramasse, N. McEvoy, W. J. Blau, J. Wang, G. Abellan, F. Hauke, A. Hirsch, S. Sanvito, D. D. O'Regan, G. S. Duesberg, V. Nicolosi, J. N. Coleman, *Nat. Commun.* **2015**, *6*, 8563.
[115] A. Rockett, *The Materials Science of Semiconductors*, Springer, US **2007**.
[116] V. Artel, Q. Guo, H. Cohen, R. Gasper, A. Ramasubramaniam, F. Xia, D. Naveh, *NPJ 2D Mater. Appl.* **2017**, *1*, 6.
[117] V. Tayari, N. Hemsworth, I. Fakih, A. Favron, E. Gaufrès, G. Gervais, R. Martel, T. Szkopek, *Nat. Commun.* **2015**, *6*, 7702.
[118] J. D. Wood, S. A. Wells, D. Jariwala, K.-S. Chen, E. Cho, V. K. Sangwan, X. Liu, L. J. Lauhon, T. J. Marks, M. C. Hersam, *Nano Lett.* **2014**, *14*, 6964.
[119] S. M. Kim, A. Hsu, M. H. Park, S. H. Chae, S. J. Yun, J. S. Lee, D.-H. Cho, W. Fang, C. Lee, T. Palacios, M. Dresselhaus, K. K. Kim, Y. H. Lee, J. Kong, *Nat. Commun.* **2015**, *6*, 8662.
[120] T. Low, R. Roldán, H. Wang, F. Xia, P. Avouris, L. M. Moreno, F. Guinea, *Phys. Rev. Lett.* **2014**, *113*, 106802.
[121] T. Low, Y. Jiang, F. Guinea, *Phys. Rev. B* **2015**, *92*, 235447.
[122] D. Xiao, G.-B. Liu, W. Feng, X. Xu, W. Yao, *Phys. Rev. Lett.* **2012**, *108*, 196802.
[123] X. Xu, W. Yao, D. Xiao, T. F. Heinz, *Nat. Phys.* **2014**, *10*, 343.
[124] K. F. Mak, K. L. McGill, J. Park, P. L. McEuen, *Science* **2014**, *344*, 1489.
[125] D. Xiao, W. Yao, Q. Niu, *Phys. Rev. Lett.* **2007**, *99*, 236809.
[126] R. V. Gorbachev, J. C. W. Song, G. L. Yu, A. V. Kretinin, F. Withers, Y. Cao, A. Mishchenko, I. V. Grigorieva, K. S. Novoselov, L. S. Levitov, A. K. Geim, *Science* **2014**, *346*, 448.
[127] M. Sui, G. Chen, L. Ma, W.-Y. Shan, D. Tian, K. Watanabe, T. Taniguchi, X. Jin, W. Yao, D. Xiao, Y. Zhang, *Nat. Phys.* **2015**, *11*, 1027.
[128] Y. Shimazaki, M. Yamamoto, I. V. Borzenets, K. Watanabe, T. Taniguchi, S. Tarucha, *Nat. Phys.* **2015**, *11*, 1032.